Polyhedron 257 (2024) 117024

Contents lists available at ScienceDirect

Polyhedron

journal homepage: www.elsevier.com/locate/poly

Bioactivity, crystal and molecular structure of vanadyl(III) complex with N-salicyloyl − N'(3,5-ditertbutyl-2-hydroxy)benzylidene hydrazine

Perizad Amrulla Fatullayeva [a,*], Ajdar Akper Medjidov [a], Marina Gennadievna Safronenko [b], Victor Nikolaevic Khrustalev [b,c], Rayyat Huseyn Ismayilov [a], Mahammad Allahverdi Bayramov [d], Bahattin Yalcin [e], Nastaran Sadeghian [f], Parham Taslimi [f], Burak Tuzun [g]

[a] Institute of Catalysis and Inorganic Chemistry, Ministry of Science and Education of the Republic of Azerbaijan, Baku, Azerbaijan
[b] People's Friendship University of Russia (RUDN University), 6 Miklukho-Maklay Street, Moscow 117198, Russian Federation
[c] N.D.Zelinsky Institute of Organic Chemistry, Russian Academy of Sciences, Leninsky Prospekt 47, Moscow 119991, Russian Federation
[d] Institute of Radiation Problems, Ministry of Science and Education of the Republic of Azerbaijan, Baku, Azerbaijan
[e] Department of Chemistry, Marmara University, Istanbul, Turkiye
[f] Department of Biotechnology, Faculty of Science, Bartin University, 74100 Bartin, Turkiye
[g] Department of Chemistry, Faculty of Science, Cumhuriyet University, 58140 Sivas, Turkiye

ARTICLE INFO

Keywords:
Hydrazones
Salicylic acid hydrazide
Thermal analysis
Complexes VO(III)
X-ray diffraction
Molecular docking

ABSTRACT

N-salicyloyl-N'-(3,5-ditertbutyl-2-hydroxy)benzylidene hydrazine (H_3sahz) and its complex with VO(III) have been synthesized. The molecular and crystal structure of the $[(VO)_2(sahz)_2(C_2H_5O)_2(C_2H_5OH)]$ complex by X-ray diffraction, as well as IR and electronic spectra, EPR spectrum etc., have been studied. The structure of the investigated VO(III) complex consists of binuclear units in which the monomeric complex molecules are linked to each other through vanadyl oxygen atom. Monomeric complexes differ between themselves in the character of coordination. Both vanadium atoms have a distorted octahedral environment. The biological activity of this compound has been studied. Lastly, the activities of the studied ligand against various enzyme proteins including acetylcholinesterase (AChE), butrylcholinesterase (BChE) and α-glycosidase (α-Gly) enzyme were compared. ChE inhibitory activities of the new complex against α-Gly, AChE and BChE were determined by Tao and Ellman's methods. The new complex was shown to have IC50 values of 42.60 μM for BChE, 91.43 μM for AChE, and 196.49 μM for α-glycosidase.

1. Introduction

Vanadium compounds have antibacterial, antiflammatory, antiviral, antifungal, antitumor, and antipyretic properties [1–8]. Vanadium compounds are also known to be used in oncological immunotherapy [9]. Among the various compounds of vanadyl with organic ligands, complexes of hydroxyaromatic hydrazones of carboxylic acid hydrazides may be of considerable interest because they contain biologically active azomethine groups (Schiff bases) and a hydrazide moiety. A series of vanadium complexes with tridentate ligands derived from 2-hydroxybenzaldehyde and various hydrazides [10,11] showed physiological activity, in particular, antidiabetic activity, which depended on the structure of the ligand. Hydrazones of terephthalic acid dihydrazide form binuclear complexes with VO(II) ions, which have catalytic activity in the oxidation of hydrocarbons [12].

The hallmarks of Alzheimer's disease (AD), a neurodegenerative condition that progresses over time, include impairments in the cholinergic system and the build-up of beta amyloid (Aβ) in the form of amyloid plaques and neurofibrillary tangles. The cholinergic system has been targeted in the development of anti-Alzheimer's medications due to its significant involvement in the control of learning and memory processes [13]. Through the inhibition of the acetylcholinesterase (AChE) enzyme, which hydrolyzes acetylcholine, cholinesterase inhibitors directly improve cholinergic transmission. Moreover, it has

* Corresponding author.
E-mail addresses: pfatullayeva43@gmail.com (P. Amrulla Fatullayeva), ajdarmedjidov@gmail.com (A. Akper Medjidov), safronenko_mg@rudn.university (M. Gennadievna Safronenko), vnkhrustalev@gmail.com (V. Nikolaevic Khrustalev), ismayilov.rayyat@gmail.com (R. Huseyn Ismayilov), mamedamea@gmail.com (M. Allahverdi Bayramov), byalcin@marmara.edu.tr (B. Yalcin), n.sadegian65@yahoo.com, nsadegian@bartin.edu.tr (N. Sadeghian), parham_taslimi_un@yahoo.com (P. Taslimi), theburaktuzun@yahoo.com (B. Tuzun).

https://doi.org/10.1016/j.poly.2024.117024
Received 26 January 2024; Accepted 3 May 2024
Available online 9 May 2024

Table 1
Crystal data and structure refinement for $C_{50}H_{68}N_4O_{11}V_2$.

Compound	$[(VO)_2(sahz)_2(C_2H_5O)_2(C_2H_5OH)]$
Empirical Formula	$C_{50}H_{68}N_4O_{11}V_2$
Molecular Weight	1002,96
Temperature	100 (2) K
Wavelength	0.71073
Space group	$P2_12_12_1$
Crystal. system	orthorhombic
a / Á	12.0544(2)
b / Á	15,0441 (3)
c / Á	27,9604 (5)
α / °	90°.
β / °	90°
γ / °	90°
Volume	5070,55 (16)
Z	4
D_{calc} g cm^{-3}	1,314
Absorption coefficient /mm^{-1}	0,430 mm^{-1}
F(000)	2120
Crystal size mm	0,32 x 0,04 x 0,04 mm^3
Angle range θ / ^{0}	2.165 to 30.516°
Number of measured reflections	65,514
Number of independent reflections	15,482 [R (int) = 0,0821]
Number of reflections with $I > 2\sigma(I)$	12,375
R-factor values($I > 2\sigma(I)$)	R1 = 0,0414, w$R2$ = 0,0788
R-factor values (all data)	R1 = 0,0637, w$R2$ = 0,0871

been shown that during the initial phases of senile plaque development, acetylcholinesterase and butrylcholinesterase (BChE) both contribute significantly to Aβ-aggregation [14]. On the other hand, an unsettling number of people worldwide are developing diabetes mellitus, a multifactorial health condition. The primary causes of diabetes's high death rates include cardiovascular illnesses, kidney impairment, and neuropathy. Alpha-amylase and alpha-glucosidase, two enzymes that catalyze the intestinal breakdown of starch, are a useful therapeutic target for reducing hyperglycemia linked to type-2 diabetes [15,16].

We have synthesized a binuclear complex OV(III) with N-(3,5-ditertbutyl-2-hydroxybenzylidene) salicyloylhydrazone, studied its crystal and molecular structure, IR and electronic spectra, etc., as well as its biological activity. The activities of the studied ligand and complex against various enzyme proteins that are AChE (PDB ID: 4M0E) have been studied. [17] and with BChE (PDB ID: 5NN0) [18], α-Gly (PDB ID: 1T0O) [19] have been compared.

2. Experimental

IR spectra were recorded on a Nicolet IS10 FTIR spectrophotometer in KBr tablets in the range of 4000–400 cm^{-1} in vaseline oil. Electronic spectra were recorded on Evolution-60S spectrophotometer, EPR spectra were recorded in the solid state at room temperature on a Bruker BioSpin GmbH radiospectrometer. NMR spectra were recorded on a Bruker 300 Hz instrument. Thermogravimetric measurements were carried out on NETZSCH STA 449F3 derivatograph, elemental analyzes were carried out at Tubitak Analytical Laboratory (Ankara) on LECOCHNS 932 analyzer. Salicylic acid hydrazide was obtained according to the procedure [20].

Obtaining the Schiff base from salicylic acid hydrazide and 3,5-di-*tert*-butyl salicylaldehyde $[(H_3sahz)_2{\cdot}(dtbsa)]$

To 1.52 g (0.01 mol) of salicylic acid hydrazide dissolved in 20 ml of ethanol was added 2.34 g (0.01 mol) of 3,5-di-*tert*-butyl-salicylic aldehyde in 25 ml of ethanol. The reaction mixture was heated to boiling and allowed to crystallize at room temperature. Yellow crystals precipitated, which were separated and dried. M.p. = 234-235°C.(971.25); C 71.74 (calc. 71.60); H 7.61 (7.48); N 7.61 (7.54)%.

Preparation of OV(III) complex with ligand $[(H_3sahz)_2{\cdot}(dtbsa)]$

A mixture of 10^{-3} mol (0.369 g) H_3sahz in 20 ml of ethanol and 10^{-3} mol (0.217 g) of $VOSO_4$ dissolved in 10 ml of water was stirred on a magnetic stirrer at a temperature of 40-50°C for 15–20 min. When remaining for a long time, dark brown crystals suitable for X-ray diffraction analysis precipitated. M.p. > 250°C (1002,96); C 59.90 (calc. 59.85); H 6.67(6.78); N5.60 (5.58); V10.15. (10.08)%.

NMR spectra

^{1}H NMR(300 MHz, CD_3OD,δ (ppm) 9.05(s, 2H, CH = N), 8.08(d., J = 8.3, 2H,Aryl-H), 7.74 (s.2H, Aryl-H), 7.59(s, 2H,Aryl-H), 7.58(s, 2H, Aryl-H), 7.092(s,2H, Aryl-H), 7.07(s,2H, Aryl-H), 3.61(q,6H, J = 6.7 Hz, ethoxy CH_2-O), 1.508 s, 18H, *t*-buthyl), (1.392, s, 18H, *t*-buthyl), 1.188 (t,9H, J = 6.7 Hz, CH_2CH_2-H,ethoxy). (The ^{1}H NMR spectra are shown in Fig. 4).

^{13}C NMR(300 MHz, CD_3OD, δ (ppm), 27(s),30(s), 34.4(1C,s), 31.08 (1C,s), 114.1(1C,s), 116,8 (1C,s), 118.9(1C,s), 124.6(1C,s), 127.4 (1C,s), 128.1(1C,s), 128.4(1C,s), 129.4(1C,s), 136.0(1C,s), 143.1 (1C,s), 147.1 (1C,s), 158.4 (1C,s), 159.8 (1C,s),161.7(1C,s).

Cholinesterase assay

ChE inhibitory abilities of the novel compound against AChE and BChE were determined by Ellman's method and this method was based on previous studies. Inhibitions of these enzymes were evaluated spectrophotometrically at a wavelength of 412 nm [21].

3. α-Glucosidase inhibition studies

α-Glucosidase inhibitory abilities of novel compound was determined according to the reported method by Tao et al. and this method was based on previous studies. The absorbance was spectrophotometrically measured at 405 nm [22].

4. Theoretical calculations

A technique exists for contrasting the biological actions of the ligand and its metal complexes with those of enzymes. Molecular docking is the most typical of them. Metal complexes can be compared using a few of these molecular docking techniques. The HEX software is employed in this investigation. These enzyme proteins interact with the ligand and its metal complexes to boost their biological activity [23]. Molecules' biological activities were compared to those of enzymes using molecular docking calculations. Using the optimized molecule's structure and the Gaussian software, a file with the.pdb extension was produced [24]. At HEX 8.0.0, the enzyme and molecule files were examined [25]. For docking, the following variables are used: Correlation typeshape only, 3D FFT mode, 0.6-dimensional grid, 180-degree receptor and ligand ranges, 360-degree twist range, and 40-degree distance range.

5. Results and discussion

In metal complexes with various ligands, the vanadium ion can be in various oxidation states – II, III, IV and V. The V (II) and V (III) states are unstable and easily oxidized to higher oxidation states. At the same time, V(IV) in the form of vanadyl VO(II) is quite stable, although under certain conditions it can transform into the vanadate anion $[VO_3]^-$. In particular, in the synthesis of a number of complex compounds using a vanadyl salt as the starting material, dioxovanadium compounds VO(II) are formed instead of the expected vanadyl complexes. Note also that the interaction of vanadyl ions with salicylhydrazones of salicylic acid hydrazide results in the formation of both tetravalent vanadium compounds VO(II) and pentavalent vanadium VO(III)[11]. In this work, it is shown that the interaction of vanadium sulfate with *N*-salicyloyl-N′-2-hydroxy-3,5-ditertbutyl benzylidene gives VO(III) complexes with this ligand. Tables of atomic coordinates, bond lengths, valent and torsion angles, and anisotropic displacement parameters for $[(VO)_2(sahz)_2(-C_2H_5O)_2(C_2H_5OH)]$ deposited in the Cambridge Structural Data Bank. The complex $[(VO)_2(sahz)_2(C_2H_5O)_2(C_2H_5OH)]$ crystallizes in the space group P $2_12_12_1$(Table 1). The structure of the complex consists of binuclear units interconnected in the crystal lattice by intermolecular hydrogen bonds.

The binuclear structure of the vanadyl complex is built from two

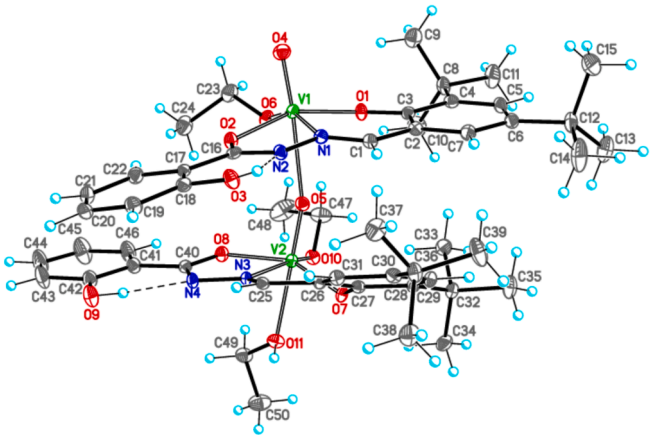

Fig. 1. Molecular structure of the complex $[(VO)_2(sahz)_2(C_2H_5O)_2(C_2H_5OH)]$.

nonequivalent monomeric complexes. In both cases, the vanadium ion is in the 5 + oxidation state. In one of the monomeric units, the vanadium (V2) ion is coordinated in the equatorial plane by three oxygen atoms: O7 (phenolic oxygen of the ditretbutylphenol fragment), enol O8-hydrazide oxygen, and O10 (oxygen of deprotonated ethanol). The fourth position is occupied by the atom of the azomethine group –CH = N-. Two oxygens are located in the axial position – the oxygen of the alcohol molecule and the vanadyl oxygen. For the V1 atom, the coordination in the equatorial plane is the same as for V2, however, the coordination in the axial position, along with the "vanadyl" oxygen, is carried out not by the ethanol molecule, but by the vanadyl oxygen of the neighboring molecule. The length of this bond, 2.471(2), is noticeably longer than for ordinary bonds, however, it is sufficient for the formation of a binuclear complex. Thus, in the binuclear structure, monomeric complexes differ from each other in the coordination character. (Fig. 1 and Scheme 1). Both vanadium atoms V1 and V2 in the binuclear formation have a distorted octahedral environment.

The bond lengths and angles are given in Table 2. The V1 = O (vanadyl oxygen) bond length is 1.585(2) Å and is close in value to that previously found [11,17]. The shortest bond in the equatorial V-O plane is observed for the bond of vanadium with the ethanol-1 anion, which has a value of 1.767(2) Å. The bond length of vanadium with the oxygen of the deprotonated hydroxyl group of the ditertbutylsalicylic fragment is 1.835(2) Å, and with hydrazide oxygen it is much longer than 1.96 Å. The bond length V(1)-N(1) (azomethine nitrogen) is 2.114(2) Å. For the V(2) ion, the lengths of these bonds are either equal or somewhat higher. There are also short distances between vanadyl oxygen VO(2) and 3 oxygen atoms and one nitrogen atom located in the equatorial plane V1:

In the dimeric molecule of the complex (Fig. 1 and Scheme 1), the ligands are in the *cis*-position with respect to each other, i.e. ditertbutylphenol fragments in both cases are directed in the same direction. The same is observed for salicyloyl fragments. Comparison of the structures of the complex of vanadyl with salicyloyl hydrazone obtained in this work and similar complexes described in the literature [8,11] shows their general tendency to bind alcohol molecules in the deprotonated form. As in similar complexes [11], the phenolic oxygen of the salicyloyl fragment does not participate in coordination with the vanadium ion.

Relatively strong intramolecular and intermolecular hydrogen bonds

Table 2
Bond lengths [Å] and angles [°] for $[(VO)_2(sahz)_2(C_2H_5O)_2(C_2H_5OH)]$.

Bond lengths [Å]	Angles [°]
V(1)-O(4) 1.585(2)	O(4)-V(1)-O(6) 103.92(10)
V(1)-O(6) 1.767(2)	O(4)-V(1)-O(1) 103.09(10)
V(1)-O(1) 1.8352(17)	O(6)-V(1)-O(1) 101.01(9)
V(1)-O(2) 1.9612(19)	O(4)-V(1)-O(2) 96.90(9)
V(1)-N(1) 2.114(2)	O(6)-V(1)-O(2) 93.53(9)
V(2)-O(5) 1.6027(19)	O(1)-V(1)-O(2) 151.51(9)
V(2)-O(10) 1.7827(19)	O(4)-V(1)-N(1) 98.08(10)
V(2)-O(7) 1.8352(19)	O(6)-V(1)-N(1) 156.29(9)
V(2)-O(8) 1.9661(18)	O(1)-V(1)-N(1) 82.26(9)
V(2)-N(3) 2.123(2)	O(2)-V(1)-N(1) 74.93(8)
V(2)-O(11) 2.261(2)	O(5)-V(2)-O(10) 101.56(10)

Table 3
Geometry of hydrogen bonds for the V(V) complex (Á).

D-H•••A	d(D-H)	d(H•••A)	d(D•••A)	< DHA
O(3)-H(3)…N(2)	0.81(4)	1.83(4)	2.571(3)	151(3)
O(9)-H(9)…N(4)	0.87(4)	1.86(4)	2.613(3)	143(3)
O(11)H(11)…O(3)#1	0.71(3)	2.09(3)	2.802(3)	175(4)

Symmetry transformations used to create equivalent atoms: #1 x + 1/2, −y + 3/2, −z + 1

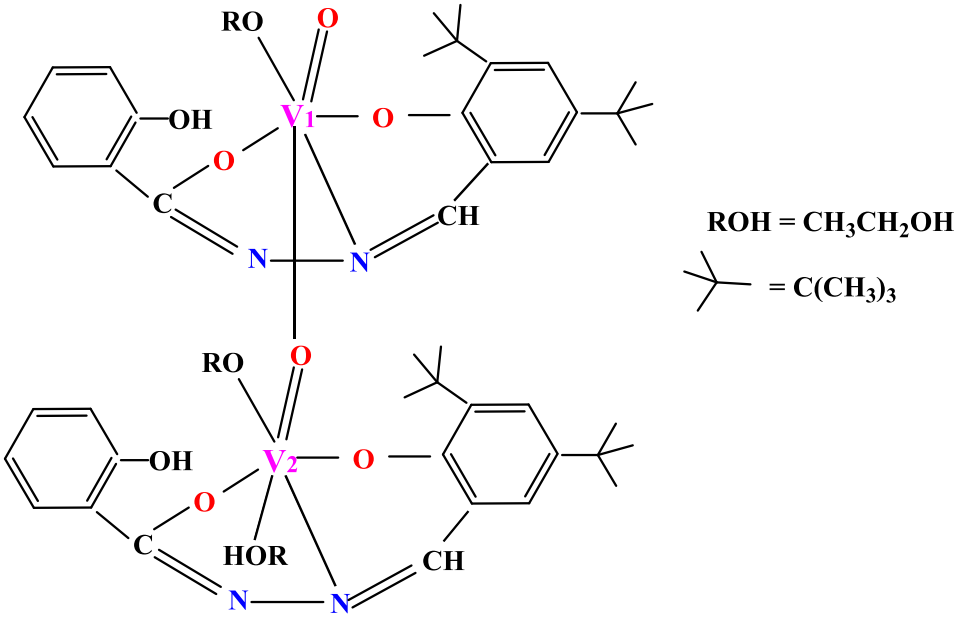

Scheme 1.

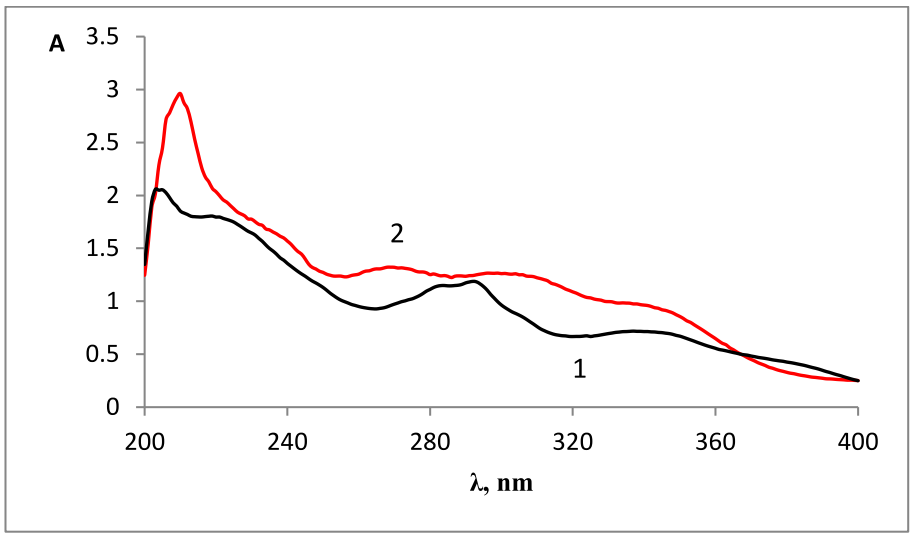

Fig. 2. Electronic spectra of the 1-ligand, 2-complex $[(VO)_2(sahz)_2{\cdot}(C_2H_5O)_2(C_2H_5OH)]$ in ethanol solution.

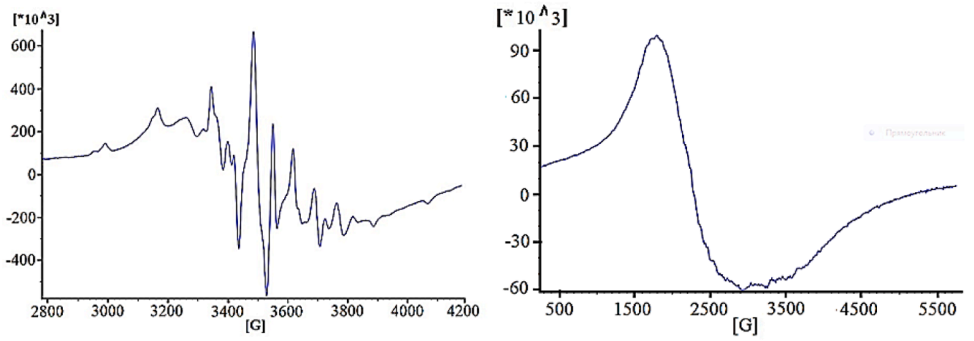

Fig. 3. EPR spectrum of a) – polycrystalline complex, b) – solution of $[(VO)_2(sahz)_2{\cdot}(C_2H_5O)_2(C_2H_5OH)]$, in toluene at 298 K.

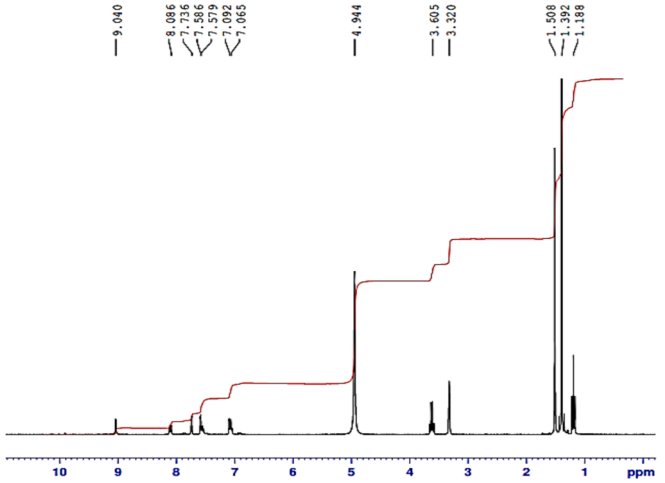

Fig. 4. ^{1}H NMR spectr of $[(VO)_2(sahz)_2(C_2H_5O)_2(C_2H_5OH)]$ in CD_3OD.

are observed (Table 3).

IR and electronic absorption spectra of the complex $[(VO)_2(sahz)_2(C_2H_5O)_2(C_2H_5OH)]$

In the IR spectrum of the studied vanadyl complex, the absorption

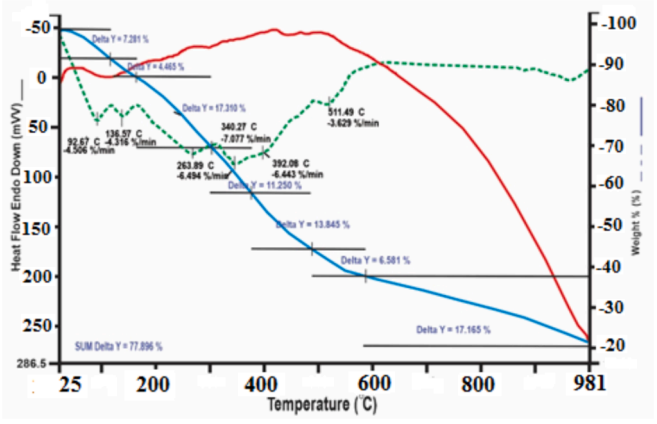

Fig. 5. Derivatogram of the complex $[(VO)_2(sahz)_2(C_2H_5O)_2(C_2H_5OH)]$.

Table 4
E total energy parameter.

	AChE	BChE	α-Gly
V metal complex	−171.79	−393.42	−367.48

Table 5
Hydrophobic Interactions of protein and metal complex.

Index	Residue	AA	Distance	Ligand atom	Protein atom
AChE protein- V metal complex					
1	441B	LEU	3.91	11,617	9202
BChE cancer –V metal complex					
1	233A	VAL	2.72	5794	2178
2	233A	VAL	3.31	5755	2177
3	361A	VAL	3.60	5833	3400
4	527A	PRO	3.22	5780	5107
α-Gly-metal complex					
1	169A	ALA	3.47	4601	1522
2	171A	PRO	3.28	4588	1536
3	173A	TYR	3.59	4597	1547
4	209A	ASP	3.94	4571	1899

In table: LEU: Leucine, VAL: Valine, PRO: Prolin, ALA: Alanin, TYR: Tirozin, ASP: Aspartic acid.

band of the C═O group of the hydrazide fragment is located at 1625 cm^{-1}, which is noticeably lower than the absorption frequency of C═O in the initial ligand (1634 cm^{-1}). The band of stretching vibrations N—H hydrazide appears at 3205 cm^{-1}, in the original ligand it is observed at 3196 cm^{-1}, i.e. it also shifts, however, in this case towards high frequencies. This situation occurs when, in coordination with the ion metal, the neighboring group enters, in this case the C═O group. A broad intense band at 3400 cm^{-1} can be attributed to the phenolic hydroxyl group and the hydroxyl group of ethanol, linked by hydrogen bonds. The absorption of the V = O group is observed at 991 and 957 cm^{-1} for VO1 and VO2, respectively.

In the electronic absorption spectra of the ligand and the complex, a number of bands associated with π-π* and n-π* transitions are observed. In the complex, these bands are hypsochromic relative to the same ligand bands (Fig. 2).

At the same time, the absorption band of the aromatic ring observed in the ligand at 203 nm shifts in the complex and is located at 209 nm. The weak absorption at 430 nm (inflection) in the absorption curve can be attributed to the charge transfer band. Thus, the data of X-ray diffraction analysis indicate the oxidation state of vanadium + 5, and, accordingly, the coordination of the carbonyl group CO in the hydrazide group –HN-NH-CO in the form of the enol form –HN-N═C-O-.

EPR spectra

The EPR spectrum of this complex contains a rather strong signal related to the tetravalent vanadium complex. To record the EPR spectra,

Table 6
Hydrogen Bonds of protein and metal complex.

Index	Residue	AA	Distance H-A	Distance D-A	Donor angel	Protein donor?	Side chain	Donor Atom	Acceptor Atom
BChE cancer –V metal complex									
1	230A	PRO	2.21	2.85	120.86	X	X	5769 [Npl]	2147 [O2]
2	233A	VAL	3.00	3.90	150.34	X	X	5808 [N3]	2176 [O2]

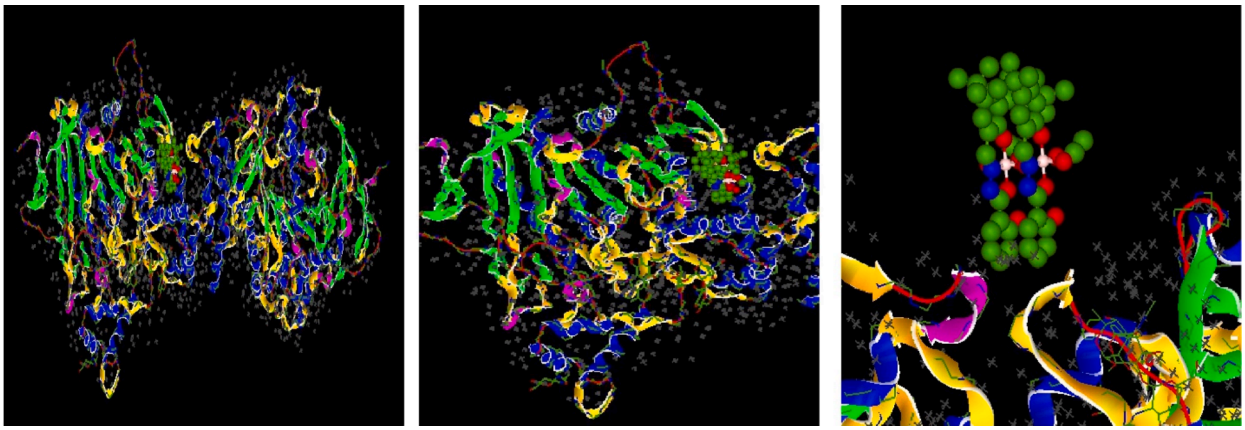

Fig. 6. Demonstration of the interaction of metal complex with AChE enzyme protein.

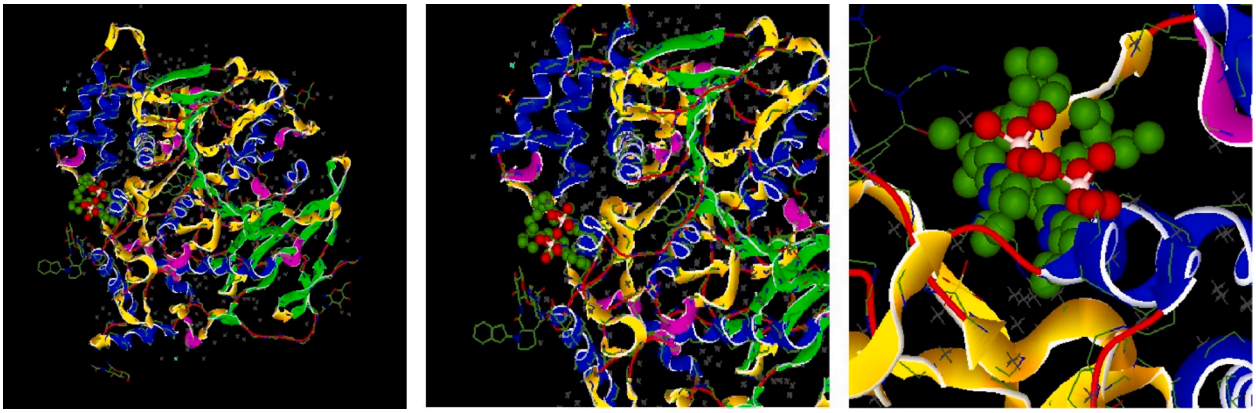

Fig. 7. Demonstration of the interaction of metal complex with BChE enzyme protein.

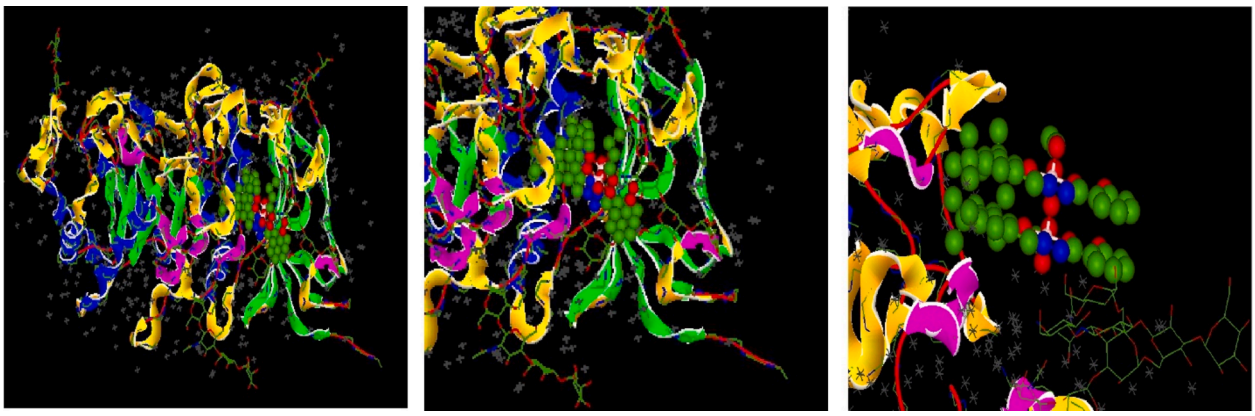

Fig. 8. Demonstration of the interaction of metal complex with α-Gly enzyme protein.

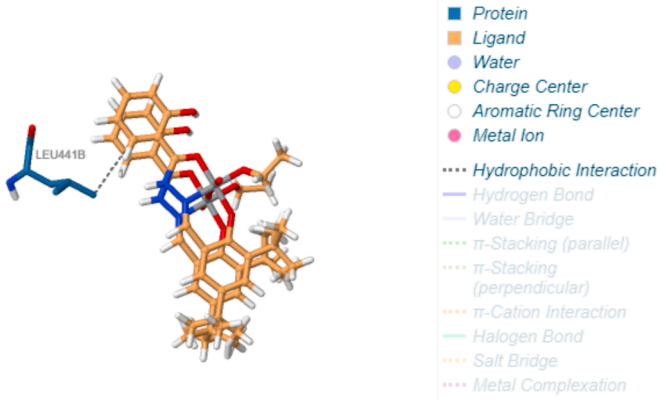

Fig. 9. Representation of the interaction of metal complex with AChE enzyme.

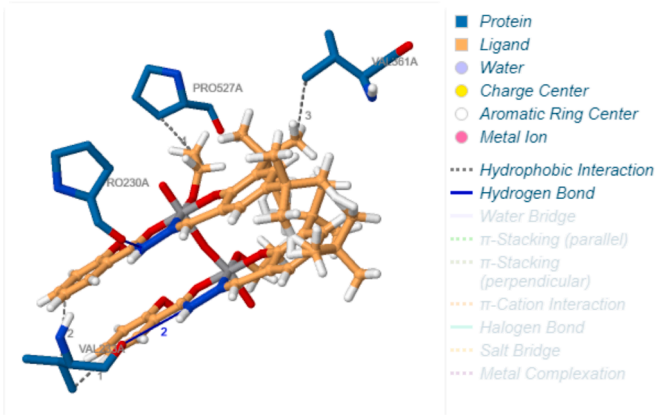

Fig. 10. Representation of the interaction of metal complex with BChE enzyme.

we used the same crystals that were used in X-ray diffraction analysis, i. e. high purity samples. This may indicate small impurities of four-vanadyl VO (II) ions, which coordinates with the ligand not through the enol, but the ketone form of the hydrazide carbonyl. The presence of complexes with the ketone form of the ligand may indicate a low rate of transition from the ketone form to the enol form during complexation and crystallization. Note, that such free ligands are in the ketone form [8] and in their vanadyl complexes in the form of the enol form [8,11,27]. For the EPR spectrum shown below (Fig. 3) of impurity complexes of tetravalent vanadyl, the following parameters were obtained:

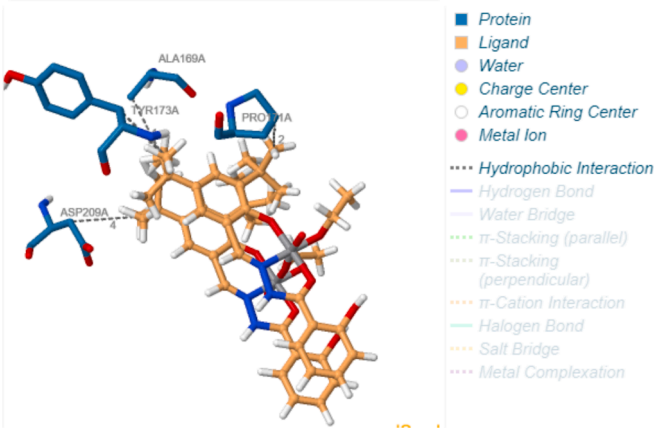

Fig. 11. Representation of the interaction of metal complex with α-Gly enzyme.

$g_{\parallel}^{1} = 1.935$ $g_{\perp}^{1} = 1.984$, $A_{\parallel}^{1} = 180\,cm^{-1}$ $A_{\perp}^{1} = 80\ cm^{-1}$

$g_{\parallel}^{2} = 1.945$ $g_{\perp}^{2} = 1.99$, $A_{\parallel}^{2} = 174\ cm^{-1}$ $A_{\perp}^{2} = 76\,cm^{-1}$

The absence of electronic absorption spectra, which could not be measured due to the very low concentration of impurity vanadyl complexes, does not allow us to assess the covalence of bonds between the metal ion and the ligand.

However, the obtained parameters of the EPR spectra made it possible to calculate the covalency of the V = O bond from the well-known equation [26].

$$\beta_2^2 = -7/6[(A\| - A_\perp)/P] + (g_e - g\|) - 5/14(g_e - g_\perp)$$

The value of the constant P characterizing the dipole interaction between the magnetic moment of the electron and the vanadium nucleus was taken equal to 126 cm^{-1}.

The obtained values β_2^2(I) = 0.8652 and β_2^2((II) = 0.8545 indicate noticeable covalency, since for a purely ionic bond the β_2^2 value is equal to unity.

In a toluene solution at 298 K (in the absence of vacuum pumping), a wide asymmetric singlet is observed. The presence of inflections in the absorption curve indicates an unresolved hyperfine structure from two vanadyl nuclei ^{51}V (the spin of the nucleus is 7 / 2).

NMR spectra

The ^{1}H NMR spectrum shows a signal at 9.05 ppm related to the imine proton. A number of peaks between 7.1–8.2 ppm are assigned to absorption of aromatic rings. The peak at 3.32 ppm can be attributed to the alcohol proton. The protons of *t*-butyl groups are observed at

chemical shifts of 1.392 and 1.508 ppm. Methyl protons of alcohol molecules are located at 1.18, and methylene ones at 3.605 ppm (Fig. 4). In the ^{13}C NMR spectra of complex absorption at 34.4 and 34.7 ppm refer to carbon atoms of *tert*-buthyl groups. The signals between δ 116.8 and 126.9 ppm belong to aromatic carbons. The signals at 156,4 ppm and 159.8 ppm refer to the carbon of the benzene ring associated with the phenolic hydroxyl group and phenolat oxygen. The signal of imine carbon (–HC = N–) is at δ 161.7 ppm.

The thermal decomposition of the complex was studied in the temperature range of 20–900 °C at a heating rate of 20 deg/min (Fig. 5).

The data of thermogravimetric analysis show that the decomposition of the complex proceeds in several stages. At the first stage (25–100 °C), a weight loss of 7.28 % occurs, accompanied by an endothermic effect and corresponding to the loss of 2 molecules of deprotonated ethanol. At the second stage, the weight loss is 4.47 % (180 °C), corresponding to the removal of the ethanolate group. The process is accompanied by an exothermic effect with a blurred maximum on the DTA curve in the region of 300 °C. The process of decomposition of the sample is completed by the loss of 88.25 % of the mass at 980 °C.

The remaining mass of vanadium dioxide 16.65 % corresponds to the metal:ligand ratio in the complex equal to 1:1. Thus, according to X-ray diffraction data, N(3,5-ditert-butylsalicylidene)-N´-salicyloyl) hydrazide forms binuclear VO(III) complexes with vanadium ions, in which the monomeric units are bonded via one vanadyl oxygen. It is shown that paramagnetic impurities are due to the presence of vanadyl complexes with ligands in the ketone form.

Study of the biological activity of the synthesized compound

Alzheimer's disease (AD) is a neurodegenerative disease noted in elderly populations with dementia, memory loss, and cognitive impairment. AChE is a key enzyme that hydrolyzes the neurotransmitter acetylcholine at cholinergic synapses in both the peripheral nervous system and the central nervous system. The α-glycosidase of the brush border mucosa of the small intestine catalyzes the digestion of starch and disaccharides in the human body. The α-glycosidase enzymes located in the small intestine brush border are especially capable of hydrolysing terminal 1 → 4-linked glucose residues to release a single α-glucose molecule [28,29].

AChE enzyme inhibitors are used in many fields. These areas are listed below; a) Naturally, poisons of vegetable and animal origin can inhibit the AChE enzyme. b) Nerve gases can be used as chemical weapons. They are found in insecticides. c) For medical purposes, it is used in the treatment of glaucoma and myasthenia gravis, as an antidote against anticholinergic poisoning, to reverse the effect of non-storing muscle relaxants, in the treatment of neuropsychiatric symptoms of diseases such as Alzheimer's, especially against unresponsiveness, in the treatment of Lewy Body Dementia and Parkinson's Diseases [30]. BChE enzyme inhibitors, like AChE inhibitors, have found an important application area in the treatment of Alzheimer's disease in recent years. ChE inhibitory activities of the new complex against α-Glu, AChE and BChE were determined by Tao and Ellman's methods. In this study, the new complex was shown to have IC50 values of 42.60 μM for BChE, 91.43 μM for AChE, and 196.49 μM for α-glycosidase. On the other hand, The Ki values of the studied complex were determined to be 201.55 μM for α-glycosidase, 88.25 μM for AChE, and 37.95 μM for BChE. Cholinesterase inhibitors, by inhibiting AChE reversibly or irreversibly, stop or slow down the hydrolysis reaction of ACh, thereby increasing the level of ACh. In this way, the low ACh level seen in Alzheimer's patients is increased to normal values. At the same time, the high AChE activity around the amyloid plaques observed in the brains of Alzheimer's patients confirms the strategy of using this group of drugs in treatment. AChE inhibitors are one of the most effective drug groups with a certain success rate in the treatment of AD today. Additionally, Alpha glycosidase inhibitors competitively reversibly bind to the enzyme, delaying carbohydrate absorption and absorption and maintaining it throughout the gastrointestinal tract. Thus, it causes a decrease in postprandial plasma glucose in both type 1 and type 2 DM [31].

Theoretical calculations

Theoretical calculations are common methods used to compare the activities of molecules. The most used method among these calculations is molecular docking, which analyzes the interactions of molecules with various proteins in the calculations made by these methods. These interactions are generally chemical interactions [32]. As these interactions increase, you can see that the activities of the molecules or their metal complexes increase. E total energy value of the calculated parameters of the studied molecules as a result of the calculations is a parameter used to compare the activities of the molecules [33]. It is known that the molecular activity with the most negative numerical value of this parameter is the highest. E total energy values of molecules calculated against various proteins are given in Table 4.

As a result of these molecular docking calculations, the activity of metal complex was compared. The chemical interactions occurring in this comparison cannot be seen in detail. PLIP analysis of it was performed. The interactions of ligand and its metal complexes with this analysis are given in Table 5 and 6 and Figs. 6-8, 9-11.

6. Conclusions

N-salicyloyl-N'-(3,5-ditretbutyl-2-hydroxy)benzylidene hydrazine [$(H_3$sahz$)_2$·(dtbsa)] forms binuclear complexes with vanadium. The binuclear structure of the vanadyl complex is built from two nonequivalent monomeric complexes. In both cases, the vanadium ion is in the 5 + oxidation state. In one of the monomeric units, the vanadium (V2) ion is coordinated in the equatorial plane by three oxygen atoms: phenolic oxygen of the ditretbutylphenol fragment, enol hydrazide oxygen, and oxygen of deprotonated ethanol. The fourth position is occupied by the atom of the azomethine group –CH = N-. Two oxygens are located in the axial position – the oxygen of the neutral alcohol molecule and the vanadyl oxygen. For the V1 atom, the coordination in the equatorial plane is the same as for V2, however, the coordination in the axial position, along with the vanadyl oxygen, is carried out not by the ethanol molecule, but by the vanadyl oxygen of the neighboring molecule(bond length 2.471 Å). It is shown that paramagnetic impurities are due to the presence of vanadyl complexes with ligands in the ketone form. The activity of the metal complex in some enzyme proteins has been studied. Afterwards, PLIP analysis was performed to examine the interaction of metal complex in more detail. Acetylcholine availability in brain areas and Aβ deposition are both increased by AChE and BChE inhibition, which has been shown to be important targets for the effective management of AD and diabetes. The complex we studied in this study can be used for drug design in future studies.

CRediT authorship contribution statement

Perizad Amrulla Fatullayeva: Investigation. **Ajdar Akper Medjidov:** Project administration. **Marina Gennadievna Safronenko:** Investigation. **Victor Nikolaevic Khrustalev:** Formal analysis. **Rayyat Huseyn Ismayilov:** Investigation. **Mahammad Allahverdi Bayramov:** Investigation. **Bahattin Yalcin:** Investigation. **Nastaran Sadeghian:** Investigation. **Parham Taslimi:** Investigation and Writing – original draft. **Burak Tuzun:** Investigation and Writing – review & editing.

Declaration of competing interest

The authors declare that they have no known competing financial interests or personal relationships that could have appeared to influence the work reported in this paper.

Data availability

No data was used for the research described in the article.

Acknowledgements

This work was funded by the Ministry of Science and Higher Education of the Russian Federation (award no. 075-03-2020-223 (FSSF-2020-0017)). The publication has been prepared with support of the RUDN University Strategic Academic Leadership Program.

Appendix A. Supplementary data

CCDC 2123668 contains the supplementary crystallographic data for $[(VO)_2(sahz)_2(C_2H_5O)_2(C_2H_5OH)]$. These data can be obtained free of charge via https://www.ccdc.cam.ac.uk/conts/retrieving.html, or from the Cambridge Crystallographic Data Centre, 12 Union Road, Cambridge CB2 1EZ, UK; fax: (+44) 1223-336-033; or deposit@ccdc.cam.ac.uk.

References

[1] J. Szklarzewicza, A. Jurowskaa, M. Hodorowicza, et al., Inorg. Chim. Acta 455 (2017) 378–389.
[2] A.A. Azza, J. Coord. Chem. 59 (2006) 157–176.
[3] J.C. Pessoa, S. Etcheverry, D. Gambino, Coord. Chem. Rev. 24–48 (2015) 301–302.
[4] D.N. Dhar, C.L. Taploo, J. Sci. Ind. Res. 41 (1982) 501–506.
[5] Y. Jia, J. Li, Construction and Application, Chem. Rev. 115 (2015) 1597–1621.
[6] P. Przybylski, A. Huczynski, K. Pyta, et al., Curr. Org. Chem. 13 (2) (2009) 124–148.
[7] S.Y. Ebrahimipour, I. Sheikhshoaie, A.C. Kautz, et al., Polyhedron 93 (2015) 99–105.
[8] Z.-Q. Sun, Yu. Shun-Feng, Xu. Xin-Lan, et al., Acta Chim. Slov. 67 (2020) 1281–1289.
[9] D. Zamarin, Mol. Ther. 26 (2018) 9–12.
[10] Appl. Organometal. Chem. 30 (2016) 221-230 (wileyonlinelibrary.com).
[11] J. Szklarzewicz, A. Jurowska, M. Hodorowicz, et al., Transit. Met. Chem. 46 (2021) 201–217.
[12] H.H. Monfared, N.A. Lalami, A. Pazio, et al., Inorg. Chim. Acta 406 (2013) 241–250.
[13] P. Taslimi, F. Akhundova, M. Kurbanova, et al., Polycycl. Aromat. Compd. 42 (9) (2022) 6003–6016.
[14] A. Altay, E. Yeniceri, P. Taslimi, et al., S. Afr. J. Bot. 150 (2022) 940–955.
[15] C.Türkeş, S. Akocak, M. Işık, et.al. 40(19), (2022) 8752-8764.
[16] M.T. Sakarya, H.İ. Gül, C., Yamali, et al . Journal of the Turkish Chemical Society Section A, Chemistry 10 (2) (2023) 385–424.
[17] U. Kosak, B. Brus, D. Knez, S. Zakelj, et al., J. Med. Chem. 61 (1) (2018) 119–139.
[18] J.Cheung, E. N.Gary, K.Shiomi, et.al. ACS medicinal chemistry letters, 4(11) (2013) 1011-1124.
[19] A.M. Golubev, R.A.P. Nagem, J.B. Neto, et al., J. Mol. Biol. 339 (2) (2004) 413–422.
[20] B.S. Furniss Vogel's, B.S.Furniss, A.J.Hannaford, P.W.G.Smith, et.al.Textbook of practical Organic Chemistry. Longman Group UK Limited, (1989) 1269.
[21] M.A. Yılmaz, P. Taslimi, Ö. Kılıç, et al., J. Biomol. Struct. Dyn. 41 (2) (2023) 445–456.
[22] D. Kısa, R. Imamoglu, N.Genc, et.al. ChemistrySelect, 8(6) (2023) e202204196.
[23] G. Kurtoglu, B. Avar, H., Zengin, et al, J. Mol. Liq. 200 (2014) 105–114.
[24] M. J. Frisch, G. W.Trucks, H. B. Schlegel, et.al. Gaussian 09 (2009) revision D.01. Gaussian Inc.
[25] D.W. Ritchie, & V.Venkatraman Bioinformatics (Oxford, England), 26(19) (2010) 2398-2405.
[26] I. Mishra, The Scientific Temper 14 (2) (2023) 445–452.
[27] L. Yanmin, X. Luao, D. Mengmeng, et al., Inog. Chem. Commun. 105 (2019) 212–216.
[28] F.S. Tokalı, P. Taslimi, M. Sadeghi, et al., ChemistrySelect (2023) e202301158.
[29] L. Durmaz, İ. Gulçin, P. Taslimi, et al., ChemistrySelect 8 (34) (2023) e202300170.
[30] F.S. Tokalı, P. Taslimi, B. Tuzun, et al., Chem. Biodivers. 20 (10) (2023) e202301134.
[31] E. Çelik, M. Özdemir, B. Köksoy, et al., ChemistrySelect 8 (38) (2023) e202301786.
[32] D. Majumdar, J.E. Philip, B. Tüzün, et al., J. Inorg. Organomet. Polym Mater. 32 (2022) 4320–4339.
[33] Ü.M. Koçyiğit, P. Taslimi, B. Tüzün, et al., J. Biomol. Struct. Dyn. 40 (10) (2020) 4429–4439.